Hindawi
Shock and Vibration
Volume 2022, Article ID 2068218, 11 pages
https://doi.org/10.1155/2022/2068218

Research Article

An Efficient Noise Elimination Method for Non-stationary and Non-linear Signals by Averaging Decomposed Components

Zhenzhou Sun,[1,2] Hongchao Lu,[3] Jiefeng Chen,[1,2] and Jialong Jiao[3,4]

[1]*Key Laboratory of Far-shore Wind Power Technology of Zhejiang Province, Hangzhou 311122, China*
[2]*Renewable Energy Engineering Institute, Power China Huadong Engineering Corporation, Hangzhou 311122, China*
[3]*School of Civil Engineering and Transportation, South China University of Technology, Guangzhou 510641, China*
[4]*State Key Laboratory of Coastal and Offshore Engineering, Dalian University of Technology, Dalian 116024, China*

Correspondence should be addressed to Hongchao Lu; luhclhc@scut.edu.cn and Jialong Jiao; jiaojl@scut.edu.cn

Received 5 October 2021; Revised 16 April 2022; Accepted 20 April 2022; Published 21 May 2022

Academic Editor: Abdollah Malekjafarian

In this paper, a moving-average method of smoothing noise based on complex exponential decomposition is applied to eliminate noise of a non-stationary signal and a non-linear signal produced by Bouc–Wen model, which are added to white Gaussian noise to simulate the noise in measured signal. The method uses a sliding window cutting the entire non-stationary and/or non-linear signal into small segments and considers that the small segments are stable and linear. The segments are decomposed into a series of components via complex exponential decomposition, and the high-energy components are reserved to reconstruct de-noised signal. Then, due to the overlap of the reconstructed segments, the average value at the same time point of reconstruction signal is regarded as the de-noised data. A non-stationary signal and a non-linear signal are selected to investigate the performance of the proposed method, the results show that the proposed method has better de-noising efficiency compared with the wavelet shrinkage method and the Savitzky–Golay filter method based on EMD (EMD-SG) for dealing with the signals with SNR of 10 dB, 15 dB, and 20 dB, and de-noised signal using the proposed method has the highest signal-to-noise ratio (SNR) and the least root mean square error (RMSE).

1. Introduction

Vibration monitoring is an important method to obtain information of operating conditions of structure, which is commonly used in mechanical engineering, and can be applied to research the vibration performance of mechanical device and monitor possible damage of structure and so on [1–5]. However, noise is an inevitable part existing in measured vibrating response data, which is induced by many factors, such as the processes generated by local and intermittent instabilities, the concurrent phenomena in the environment of data test, and the sensors, and recording systems [6]. Figure 1 shows the measured vibrating signal of an offshore substation located at the East China Sea, which indicates that the noise is obvious. The noise presenting in signal may affect the accuracy of analysis result seriously. After obtaining the vibrating data of vibrating systems, the information of the systems should be further extracted. Hilbert–Huang transform is a commonly used signal processing method, which is widely applied to deal with the vibrating signal of non-linear and time-varying system [7–9]. Empirical mode decomposition (EMD) is essential when implementing Hilbert-Huang transform, which is vulnerable for noise [10]. The study of bearing damage shows that the accuracy can be severely limited by noise [11]. Therefore, data pretreatment of de-noising is necessary to obtain accurate result of analysis when the signal is contaminated by noise.

In many applications, signal de-noising is the process of estimating the uncontaminated signal from measured data. The estimated signal should be as close as possible to the original one and contain most of its important properties [12]. Traditional de-noising schemes are usually based on linear methods, the Fourier filters are commonly used to

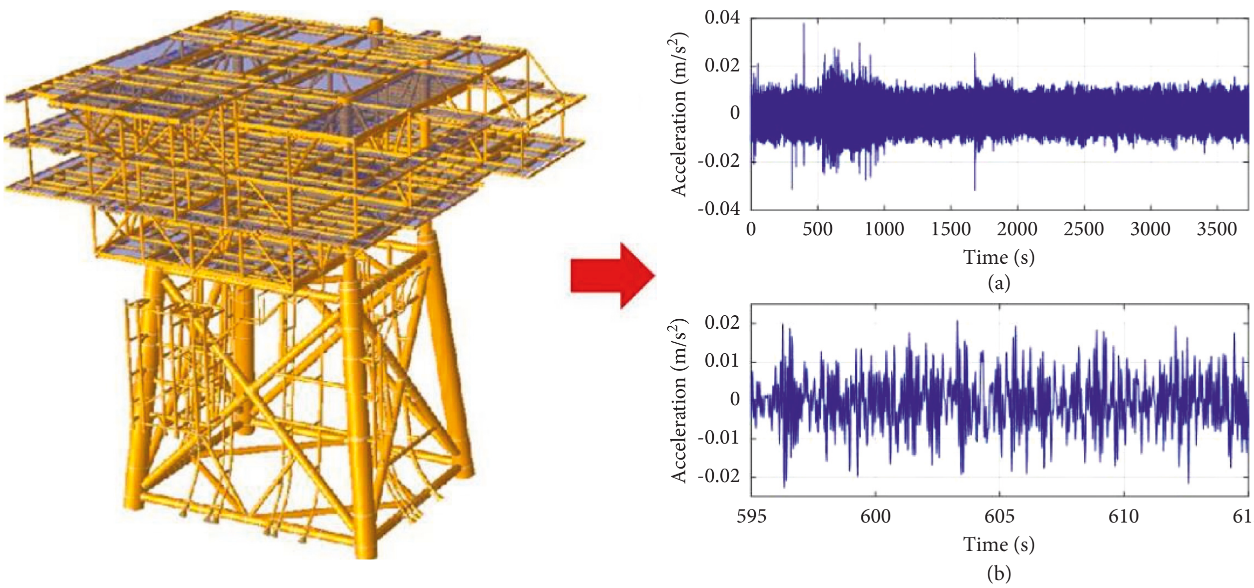

Figure 1: Measured vibrating signal of offshore substation: (a) model of offshore substation; (b) measured vibrating signal.

separate the noise from the measured signal when the data generation processes are linear and the noises have distinct time or frequency scales different from the true signal [13]. Wiener filter is another frequently used linear de-noising method, which adopts minimum value of mean square error between estimated random process and desired process as an optimal criterion [14]. Linear de-noising methods are easy to implement and to design, but they have limitations as well. The methods are not effective when signals have sharp edges and impulses in short duration [12]. Furthermore, filter methods will be failed when the processes are either non-linear or non-stationary because the filter methods are based on linear theory. One adverse effect is mixing when using filter methods to deal with non-linear signal, even though the real signal and the noises have distinct fundamental frequencies. The mixing of harmonics with noises will lead to terrible results of noise separation. Under such conditions, many non-linear de-nosing methods are proposed, especially for the methods based on wavelet thresholding and EMD. The wavelet method considers that the energy of a signal will commonly focus on a few coefficients in wavelet domain while the energy of noise is spread among all coefficients, which are relatively small in general. Donoho [15, 16] proposed the hard and soft thresholding methods for de-noising based on wavelet transform, where the former reserves coefficients if their magnitudes are larger than a given threshold, or makes other coefficients zero, while the latter just shrinks coefficients whose magnitudes are larger than threshold to zero by the threshold value. The methods are widely used to de-noising and have good results. However, the drawbacks of the hard and soft thresholding methods are obvious. The obtained coefficients using hard thresholding are discontinuous at threshold value, which may lead to the reconstruction signal oscillating. The latter makes coefficients used to reconstruct signal different from original coefficients with permanent bias, which influences the degree of the closeness between reconstructed and true signals, and brings unavoidable errors. Besides, the basis functions of wavelet approaches are fixed, which do not necessarily match the varying natures of signals.

EMD is an adaptive method proposed by Huang et al. [17], which can decompose any complicated data into a finite and often small number of intrinsic mode functions (IMFs). The IMFs become the basis representing the data, which offer a physically meaningful representation of the underlying processes. The basis functions are extracted from the original data, which means the analysis is adaptive. Since the basis is adaptive, EMD is ideally applicable to the measured data from non-linear and non-stationary processes. The sifting process of EMD starts from high frequency modes to low frequency modes with various intrinsic time scales, which signifies that the first IMFs are dominated by noise than the last ones if the analyzed signal contains noise. Based on the properties of EMD, Boudraa et al. [12] proposed a de-noising method combining with thresholding. The method of eliminating noise is based on estimated IMFs, which are obtained from sifted IMFs from original signal and threshold value. After obtaining the estimated IMFs of signal, the de-noising process is implemented by reconstructing the estimated IMFs. In addition, Flandrin et al. [18] implemented numerical experiments based on fractional Gaussian noise to understand the way of EMD behaves in stochastic situations related to broadband. Wu and Zhang [6] indicated that the EMD was an effective dyadic filter with the ability of separating the white noise into IMF components, which have mean periods exactly twice the value of the previous components. Ensemble EMD (EEMD) is a noise-assisted technique, which is applied to attenuate mode mixing and noise to some extent [19]. Rehman and Mandic [20] further investigated the behavior of EEMD in the presence of white Gaussian noise. Li and Wang [21] proposed a novel noise reduction method based on complete

EEMD, which was applied to deal with underwater acoustic signals and obtained good results. Li et al. [22] proposed a time-varying filter to implement EMD, which is robust against noise interference. Excluding the methods based on EMD, Iqbal et al. [23, 24] proposed de-noising methods based on singular value decomposition technique, which achieved promising results.

The purpose of this paper is to propose a more suitable de-noising method to deal with non-stationary and non-linear signal corrupted by noise. The method has a better de-noising efficiency and stable performance in different noise levels. In the process of de-noising using the proposed method, the original non-stationary and non-linear signal is cut into small segments, and the segments are assumed to be stable and linear. The noises in the small segments are eliminated via signal decomposition and reconstruction. Two numerical examples, a non-stationary signal and a non-linear signal produced by Bouc–Wen model, are used to investigate the performance of the proposed method, which show that the proposed method can eliminate added Gaussian white noise efficiently.

2. Preliminaries

Noise is inevitably exiting in all kinds of measured signals, which may be caused by a number of factors. As a result, the collected data are always described as an amalgamation of true signal and noise, which can be expressed as follows:

$$y(t) = s(t) + n(t), \tag{1}$$

where $y(t)$ is the observed signal corrupted by noise, $s(t)$ is the true signal, and $n(t)$ is the noise.

2.1. Wavelet Shrinkage Method. A measurable square integral function space $L^2(R)$ on the real axis should be defined to carry out the wavelet transform of a signal. Then, the continuous wavelet transform of a signal $f(t) \in L^2(R)$ can be expressed as follows:

$$WT(a,b) = |a|^{-1/2} \int_{-\infty}^{\infty} y(t)\psi^* \left(\frac{t-b}{a}\right) \mathrm{d}t, \tag{2}$$

where a is a temporal scale factor which reflects the periodic length of a wavelet, b is a time position factor, $\psi * (t)$ is the complex conjugate of wavelet function, and $WT(a, b)$ are the so-called wavelet coefficients.

The wavelet shrinkage method was proposed by Donoho [16], which is implemented by the following steps: Step 1: Selecting an appropriate wavelet function and decomposition level, the wavelet coefficients of signal corrupted by noise are obtained by applying wavelet decomposition using selected parameters; Step 2: Choosing a suitable threshold of wavelet coefficient τ, the obtained coefficients in Step 1 are sifted by the threshold, which includes soft-threshold and hard-threshold; Step 3: The obtained coefficients sifted by the threshold are reconstructed to eliminate the noises in signal.

2.2. Savitzky – Golay Filter Method Based on EMD. EMD is an adaptive signal analysis method first proposed by Huang et al. [17], which can be used to deal with non-linear and non-stationary signals because of the adaptive nature of the basis. The formula of EMD is expressed as follows:

$$y(t) = \sum_{i=1}^{N} \mathrm{IMF}_i(t) + r(t), \tag{3}$$

where i is the decomposition order, IMF$i(t)$ is the ith IMF, and $r(t)$ is the residue.

The Savitzky–Golay filter method is a time-domain smoothing method, which uses least squares approach to replace the original signal points with the fitted polynomial. Boudraa [12] combined the EMD and SavitzkyGolay filter (EMD-SG) to eliminate the noises in measured signal. The method decomposes the signal corrupted by noise into a series of IMFs using (3), smooths each IMFs applying SavitzkyGolay filter, and then uses the smoothing IMFs to reconstruct de-noised signal.

3. Moving-Average Method of Smoothing Noisy Signal Based on Complex Exponential Decomposition

3.1. Signal Partition Using Sliding Window and Decomposition. For a non-stationary or/and non-linear signal, it is hard to use invariant parameters to describe the signal. One solving method is dividing the signal into litter fragments and considering that the signal segments are stationary and linear. Then, the linear method is applied to deal with the de-noising problem of small fragments. Denoting the sampling interval as Δt, $t_k = k\Delta t$, the discrete digital signal y_k with $k = 0, 1, \ldots, N-1$ can be cut into small fragments using a rectangular window. To guarantee the continuity of the signal in the process of noise elimination using the proposed method, the step of sliding window is set as 1. Then, the small fragments can be expressed as

$$y_{m,n} = y_{m+n-1}, \tag{4}$$

where m is the number of signal fragments, $m = 1, 2, \ldots, N - L + 1$, and L is the length of each signal fragment; n is the number of fragments, $n = 0, 1, \ldots, L - 1$.

The obtained segment $y_{m,n}$ can be decomposed into a sum of exponential form with real-valued and/or complex-valued exponents, which is so-called Prony series expressed as follows [25]:

$$y_{m,n} = \sum_{l=1}^{p_m} \gamma_{m,l} z_{m,l}^{n}, \tag{5}$$

where p_m is the number of terms corresponding to segment $y_{m,n}$, $z_{m,l} = \mathrm{e}^{\lambda_{m,l}\Delta t}$. Since $y_{m,n}$ is a real-valued signal, $\lambda_{m,l}$ must either be real numbers or occur in complex conjugate pairs and $\gamma_{m,l}$ have the same corresponding form. Let $\lambda_{m,l} = -\alpha_{m,l} + \mathrm{j}2\pi f_{m,l}$, then $\alpha_{m,l}$ is the damping factor in seconds −1 and $f_{m,l}$ is the frequency in Hertz; j is imaginary unit. Let $\gamma_{m,l} \equiv A_{m,l}\mathrm{e}^{\mathrm{j}\theta_{m,l}}$, then $A_{m,l}$ is the amplitude and $\theta_{m,l}$ is the sinusoidal initial phase in radians associated with $\mathrm{e}^{\lambda_{m,l}t}$.

3.2. Parameters Estimation of Prony Series. Obviously, the discrete Prony series in (5) can be viewed as the general solution of a pth-order difference equation as follows:

$$\sum_{l=0}^{p_m} a_{m,l} y_{m,n+l} = 0 \quad for\, n = 0, 1, \ldots, L - p_m - 1, \tag{6}$$

where $a_{m,l}$ are real-valued constants. Without losing the generality, let $a_{m,p_m} = 1$. The characteristic equation corresponded to (6) can be expressed as follows:

$$\sum_{l=0}^{p_m} a_{m,l} z^l = 0. \tag{7}$$

As discussed in reference [25], an ill-conditioned problem would occur in the solution process of (6) using the direct method. One method of dealing with the ill-conditioned problem is converting the high-order difference equation to a first-order matrix difference equation. Thus, new auxiliary variables are introduced as follows [26]:

$$x_{1m,n} = y_{m,n}, x_{2m,n} = y_{m,n+1}, \ldots, x_{p_m m,n} = y_{m,n+p_m-1}. \tag{8}$$

Then, a first-order matrix difference equation equivalent to (6) can be obtained as follows:

$$\mathbf{x}_{m,n+1} = \mathbf{G}_m \mathbf{x}_{m,n}, \tag{9}$$

where

$$\mathbf{G}_m = \begin{bmatrix} 0 & 1 & 0 & 0 & \cdots & 0 & 0 \\ 0 & 0 & 1 & 0 & \cdots & 0 & 0 \\ 0 & 0 & 0 & 1 & \cdots & 0 & 0 \\ \vdots & \vdots & \vdots & \vdots & \ddots & \vdots & \vdots \\ 0 & 0 & 0 & 0 & \cdots & 0 & 1 \\ -a_{m,0} & -a_{m,1} & -a_{m,2} & -a_{m,3} & \cdots & -a_{m,p_m-2} & -a_{m,p_m-1} \end{bmatrix} \in R^{p_m \times p_m}. \tag{10}$$

and

$$\mathbf{x}_{m,n} = \left[x_{1m,n} \;\; x_{2m,n} \;\; \cdots \;\; x_{p_m m,n} \right]^T \in R^{p_m \times 1}. \tag{11}$$

Mathematically, the p_m roots of the characteristic equation of (7) are exactly corresponding to the p_m eigenvalues of the matrix G_m. To avoid ill-condition problem, the eigenvalue analysis of matrix G_m is implemented to determine the roots of (7).

To compute eigenvalues of matrix G_m, a Hankel matrix is introduced, which is defined as follows:

$$\mathbf{H}_m(1) = \begin{bmatrix} y_{m,k} & y_{m,k+1} & \cdots & y_{m,k+\eta-1} \\ y_{m,k+1} & y_{m,k+2} & \cdots & y_{m,k+\eta} \\ \vdots & \vdots & \ddots & \vdots \\ y_{m,k+\xi-1} & y_{m,k+\xi} & \cdots & y_{m,k+\xi+\eta-2} \end{bmatrix}, \tag{12}$$

where ξ and η are the selected row and column of the Hankel matrix.

Substituting $k=0$ into (12) and implementing the singular value decomposition of $H_m(0)$, one can obtain [27]

$$\mathbf{H}_m(0) = \left[\mathbf{U}_{m,1} \;\; \mathbf{U}_{m,2} \right] \begin{bmatrix} \mathbf{\Sigma}_{m,1} & 0 \\ 0 & 0 \end{bmatrix} \begin{bmatrix} \mathbf{V}_{m,1}^T \\ \mathbf{V}_{m,2}^T \end{bmatrix} = \mathbf{U}_{m,1} \mathbf{\Sigma}_{m,1} \mathbf{V}_{m,1}^T. \tag{13}$$

In theory, the number of non-zero singular values in (7) is equal to p_m, $\mathbf{U}_{m,1} \in R^{\xi \times p}$, $\Sigma_{m,1} \in R^{p \times p}$ and $V_{m,1} \in R^{\eta \times p}$. While noise exists in the signal, the number of non-zero singular values is larger than p_m. Because of the singular values sorting from largest to smallest, the first pm singular values are regarded as corresponding to the real signal and other singular values are set as zero, which is the de-noising approach of the proposed method.

Letting $k=1$, $\mathbf{H}_m(1)$ can be expressed as follows [25]:

$$\mathbf{H}_m(1) = \mathbf{U}_{m,1} \mathbf{\Sigma}_{m,1}^{\frac{1}{2}} \mathbf{A}_m \mathbf{\Sigma}_{m,1}^{\frac{1}{2}} \mathbf{V}_{m,1}^T. \tag{14}$$

Then, a realization of system matrix is yielded as follows:

$$\mathbf{A}_m = \mathbf{\Sigma}_{m,1}^{\frac{-1}{2}} \mathbf{U}_{m,1}^T \mathbf{H}_m(1) \mathbf{V}_{m,1} \mathbf{\Sigma}_{m,1}^{\frac{-1}{2}}. \tag{15}$$

While the calculated eigenvalues of $\mathbf{A}_m$ are $\hat{z}_{m,l}$, $l = 1, 2, \ldots, p_m$, the corresponding $\hat{\lambda}_{m,l}$ are estimated using $\hat{\lambda}_{m,l} = \ln(\hat{z}_{m,l})/\Delta t$. Substituting $\hat{\lambda}_{m,l}$ into (5), the corresponding $\hat{\gamma}_{m,l}$ can be obtained.

3.3. Noise Elimination Using Moving-Average Method Based on the Estimated Parameters. When the parameters of Prony series are obtained, each de-noised signal segments are reconstructed by (5).

$$\hat{y}_{m,n} = \sum_{l=1}^{p_m} \hat{\gamma}_{m,l} e^{\hat{\lambda}_{m,l} n \Delta t}. \tag{16}$$

With the sliding window moving, the noises in small segments are eliminated. Due to the step of sliding window is 1, the overlap of post-segment and pre-segment is $L-1$. For the whole duration signal, the reconstructed segments at the same time point should be calculated average, which is the de-noised data at the time point. When the sliding window moves across the entire signal, the de-noised signal $\hat{y}_k$ with $k=0, 1, \ldots, N-1$ is obtained.

4. Example Studies

In this paper, two different numerical examples are applied to test the performance of the proposed de-noising method. The process and de-noising results are exhibited in detail.

4.1. Test Case 1: Non-stationary Example. In this example, a non-stationary signal is chosen to investigate the performance of proposed method. The frequency of the non-stationary signal is time varying, which is synthesized using the following formula [22]:

$$y(t) = \cos\left(20\pi t + 4\pi t^2\right) + \cos\left(4\pi t + 4\pi t^2\right). \tag{17}$$

To investigate the capability of the proposed de-noising method, the different levels of noise are added to the non-stationary signal, which is simulated using the additive model as follows:

$$y_{noi}(t) = y(t) + y_N(t), \tag{18}$$

where $y_{noi}(t)$ is the signal contaminated by noise, $y(t)$ is the clear signal, and $y_N(t)$ is the noise signal exiting in the measured signal.

For testing purposes, the white Gaussian noise is added to the clear signal to simulate the test noise of measured signal. The signal-to-noise ratios (SNRs) are set as 10 dB, 15 dB, and 20 dB. With the sampling interval $\Delta t = 0.001$ s and the number of simulation points $N = 5120$, the discrete signals with total duration of 5.12 s are obtained. For simplicity, the signal with an SNR of 10 dB is shown in Figure 2, the upper part is clear signal compared with noise signal, and the bottom part is the clear signal compared with the signal corrupted by noise.

Typically, the wavelet shrinkage and EMD-SG methods are implemented to eliminate the noise embedded in the non-stationary signal as comparisons. Hard thresholding is selected as shrinkage rule in this example, and sym8 wavelet at level 10 is applied when using wavelet shrinkage to eliminate the noise in the signal. Implementing EMD to the non-stationary signal corrupted by noise, 11 IMFs can be obtained. The SavitzkyGolay smoothing filter is applied to each IMF with an order of 5 and a frame length of 21. The comparison of de-noised signals using above two methods and clear signals is exhibited in Figure 3 (SNR = 10 dB). The figure shows that the two methods are able to smooth the embedded noise of the non-stationary signal, but the discrepancies are obvious compared with the clear signal.

To illuminate the proposed de-noising method, the comparison diagrams between clear signal and de-noised signals with the three noise levels are exhibited in Figures 4–6. When using the proposed method to deal with the signal with an SNR of 10 dB, the length of moving window is set as 160, which means that the duration of moving window used to select data is 1.6 s and the segments are regarded as linear and stationary in the procedure. With movement of the window, the non-stationary is cut into small segments, which are decomposed as linear and stationary signal. Applying Prony decomposition to the small segments and reconstructing the signal using reserved $\lambda_{m,l}$ and $\gamma_{m,l}$, the noise is removed in the procedure of decomposition and reconstruction. To demonstrate the computational efficiency of the proposed method, the elapsed time of canceling noise process is recorded. For the signal corrupted by the noise with an SNR of 10 dB, the elapsed time is 69.7 s (CPU Inter Core i7-8700, 3.2 GHz). Enlarging the de-noised signal during 3.5 s to 3.7 s, the details show that the de-noised signals using the proposed method match well with the original signals under the influence of noises with SNRs of 10 dB, 15 dB, and 20 dB.

EMD is an adaptive data analysis method, which is widely used for non-stationary and non-linear signals. However, EMD is sensitive to noise. To analyze the efficiency of proposed method further, the de-noised signal containing noise with 15 dB is decomposed into a series IMFs using EMD. The first three IMFs are extracted because the low-order IMFs contain the main information of signal. Comparing the first three IMFs of the clear and de-noised signals, the results indicated that the first IMFs match with each other well and the second and third IMFs have small discrepancies, which are shown in Figure 7.

To quantify the de-noising efficiency, the SNR and root mean square error (RMSE) are introduced as criteria to estimate the efficiency of noise reduction. Before de-noising, the SNR of the three signals are 10 dB, 15 dB, and 20 dB. The SNR and RMSE of de-noised signals using the three methods are listed in Table 1. It indicates that the SNR of de-noised signal using proposed method is maximal and the corresponding RMSE is minimal under different noise levels. Compared with the signal contaminated noise with the SNRs of 10 dB, 15 dB, and 20 dB, the SNRs are increased by 14.724 dB, 14.428 dB, and 14.688 dB using proposed method, and the corresponding RMSEs have reductions of 53.56%, 51.99%, and 53.54% compared with the better traditional method (EMD-SG), which suggests that the de-noising efficiency of proposed method is obvious.

4.2. Test Case 2: Non-Linear Example. Bouc–Wen model is a typical non-linear model to describe hysteretic phenomena, and it is encountered in many scientific fields. For example, hysteretic behavior of engineering structures often shows up under severe cyclic loads such as earthquakes, high winds, and waves. In this example, a Bouc–Wen model is selected to investigate the performance of the proposed method dealing with non-linear signal contaminated by noise since it is widely used. The following set of differential equations describes the motion of a single degree of freedom (SDOF) system with Bouc–Wen hysteresis:

$$\begin{cases} \ddot{x}(t) + 2\zeta\omega\dot{x}(t) + \gamma\omega^2 x(t) + (1-\gamma)\omega^2 z(t) = f(t), \\ \dot{z}(t) = A\dot{x}(t) - \alpha|\dot{x}(t)|z(t)|z(t)|^{n-1} - \beta\dot{x}(t)|z(t)|^n, \end{cases} \tag{19}$$

where $x(t)$, $\dot{x}(t)$ and $\ddot{x}(t)$ are the displacement, velocity, and acceleration, respectively; ζ is the damping; ω is the natural frequency; γ is the ratio of post-yield to pre-yield stiffness; $f(t)$ is the external excitation acts on the system; $z(t)$ is the hysteretic displacement; and A, n, α, β are the parameters to regulate shape of the hysteresis loop.

Letting $A = 1$, $n = 3$, $\alpha = 2.1$, $\beta = 1$, the frequency $\omega = 3$, damping $\zeta = 0.15$, and assuming that the external exaction is harmonic, $f(t) = 10\cos(0.5\,t)$ in this example, the response of the Bouc–Wen model governed by (19) can be calculated using Runge–Kutta method. With the calculation step $\Delta t = 0.01$ s and the number of computation points $N = 10000$, the response of the Bouc–Wen model with total duration of 100 s is obtained. The hysteretic loop of the system is shown as Figure 8, which reflects the non-linearity of the Bouc–Wen model.

As well as non-stationary signal above, the noises are added to the clear signal calculated by the Bouc–Wen model with the SNRs of 10 dB, 15 dB, and 20 dB, which will be used

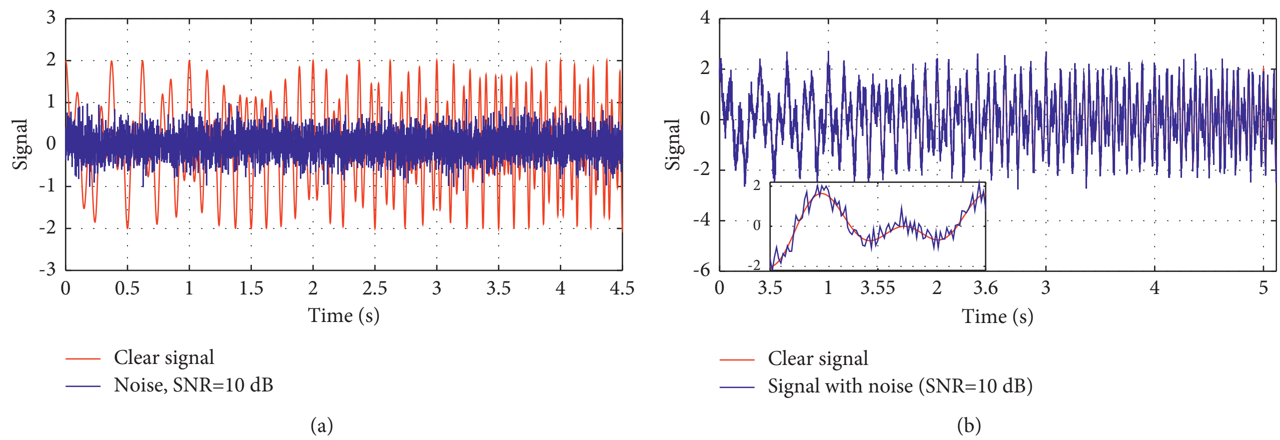

Figure 2: Non-stationary signal: (a) comparison of clear signal and noise; (b) comparison of contaminated and clear signal.

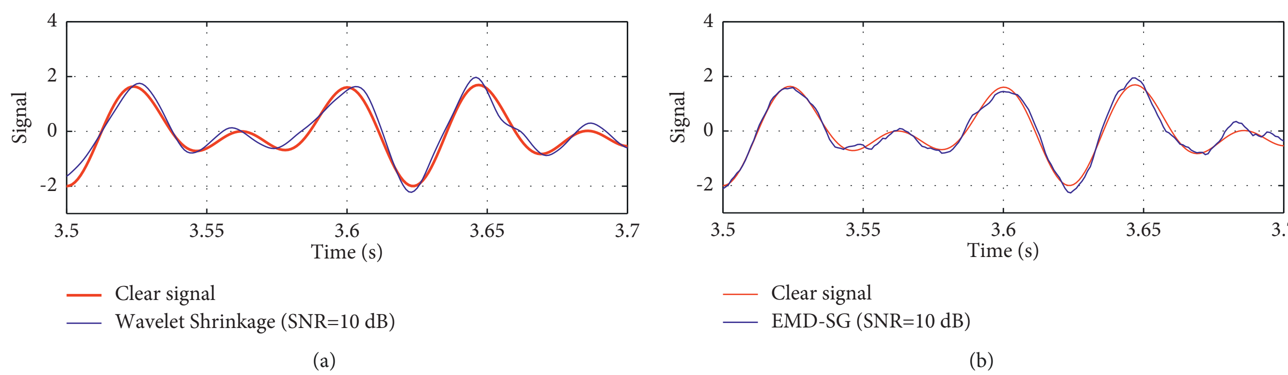

Figure 3: Noise elimination of non-stationary signal using traditional methods: (a) Wavelet shrinkage method; (b) EMD-SG method.

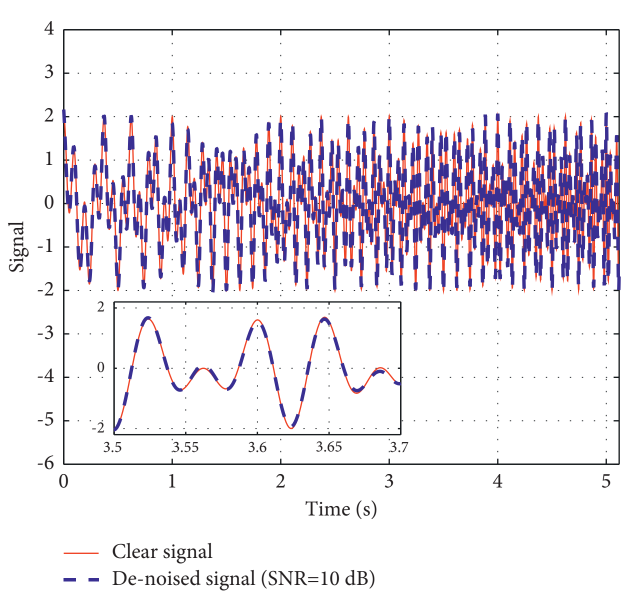

Figure 4: Noise elimination of non-stationary signal using proposed method when SNR = 10 dB.

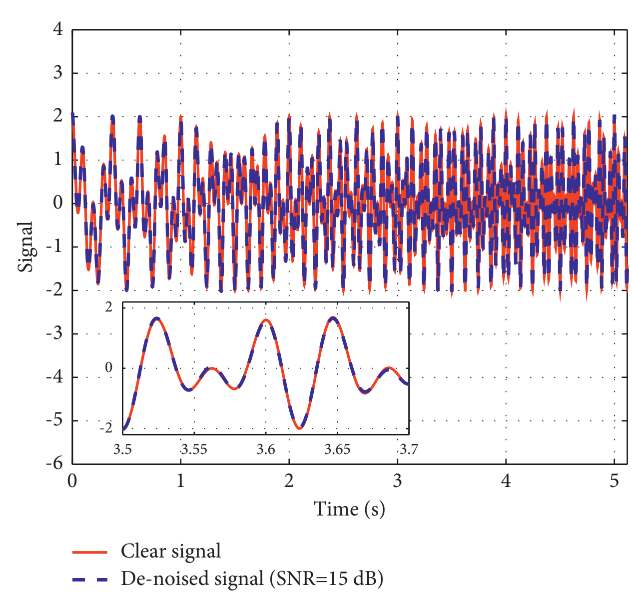

Figure 5: Noise elimination of non-stationary signal using proposed method when SNR = 15 dB.

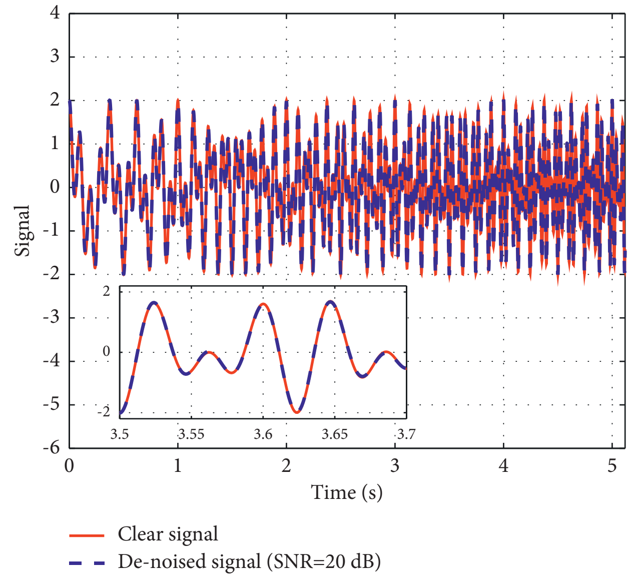

FIGURE 6: Noise elimination of non-stationary signal using proposed method when SNR = 20 dB.

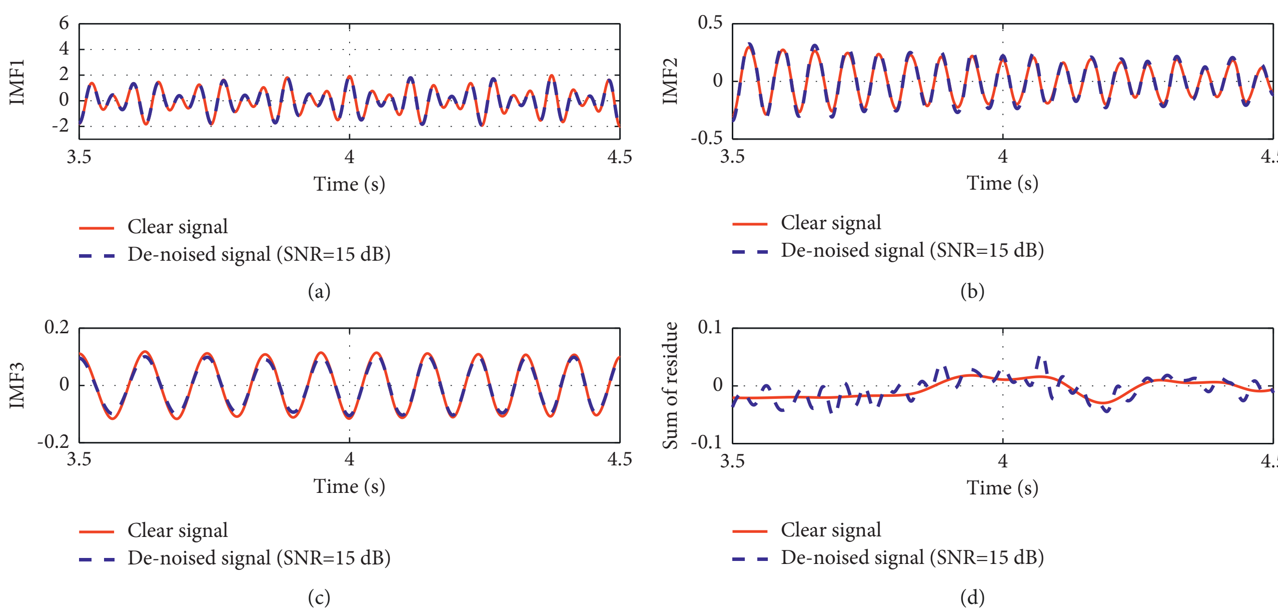

FIGURE 7: IMFs comparison between clear signal and de-noised signal using proposed method.

TABLE 1: De-noised results in SNR and RMSE of non-stationary signal corrupted by different noise levels.

Noise level	10 dB		15 dB		20 dB	
Criteria	SNR (dB)	RMSE	SNR (dB)	RMSE	SNR (dB)	RMSE
Wavelet shrinkage method	15.587	0.1663	20.970	0.0895	26.604	0.0468
EMD-SG method	18.055	0.1251	23.055	0.0704	28.056	0.0396
Proposed method	24.724	0.0581	29.428	0.0338	34.688	0.0184

to investigate the noise elimination efficiency using proposed method to non-linear signal. Acceleration response of the system corrupted by the noise with an SNR of 10 dB is shown in Figure 9, where the adverse effect is obvious compared with clear signal. Wavelet shrinkage and EMD-SG methods are used to reduce the noises, and the de-noised results of acceleration corrupted by 10% of the noise (SNR = 10 dB) applying the two methods are exhibited in

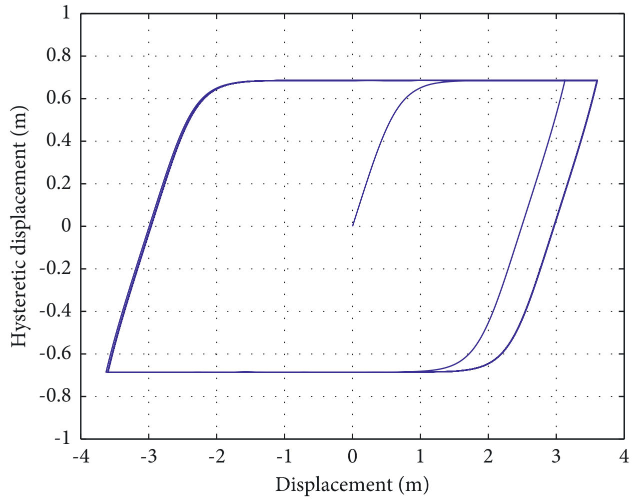

Figure 8: Hysteresis loop of the non-linear system.

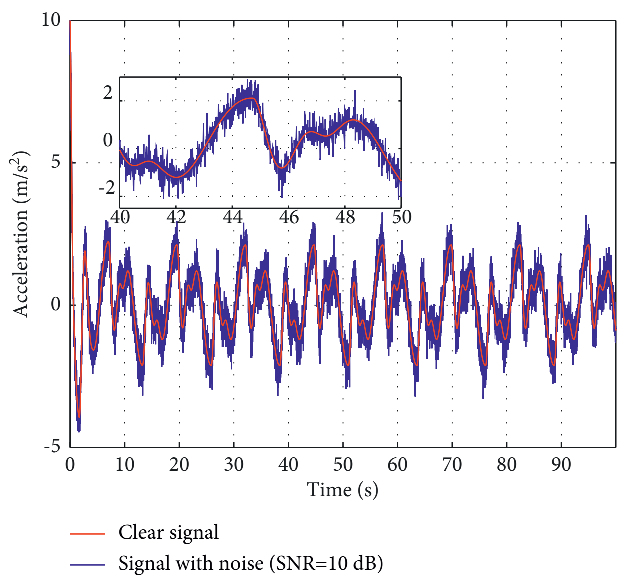

Figure 9: Comparison of clear and contaminated acceleration signals of hysteretic system.

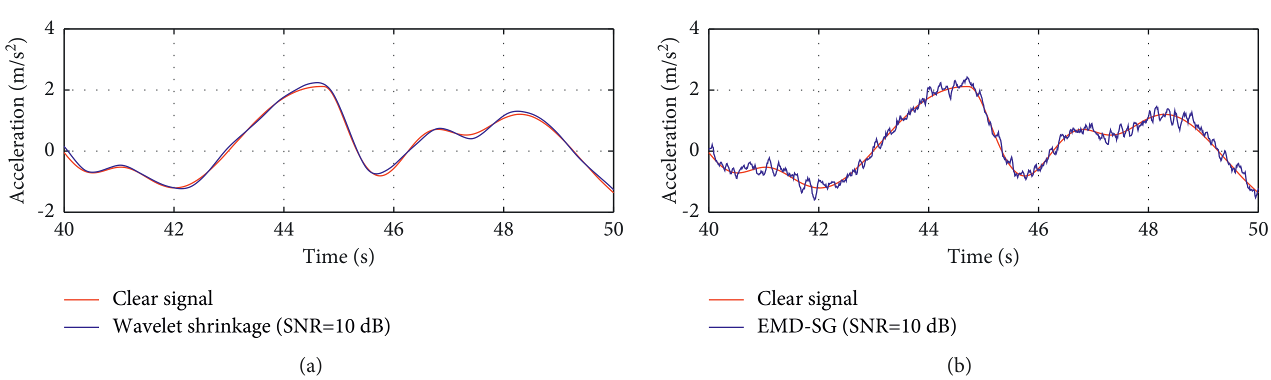

Figure 10: Noise elimination of non-linear signal using traditional methods: (a) wavelet shrinkage method; (b) EMD-SG method.

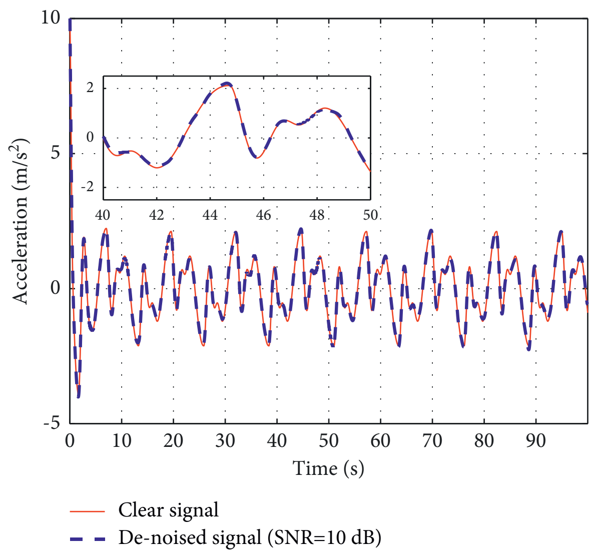

FIGURE 11: Noise elimination of non-linear signal using proposed method when SNR = 10 dB.

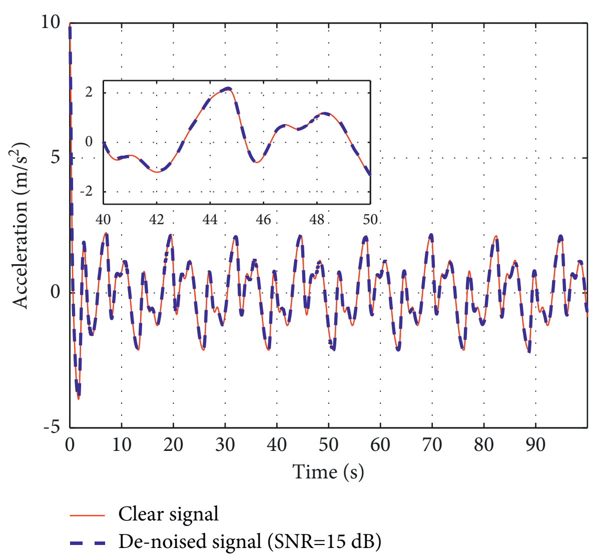

FIGURE 12: Noise elimination of non-linear signal using proposed method when SNR = 15 dB.

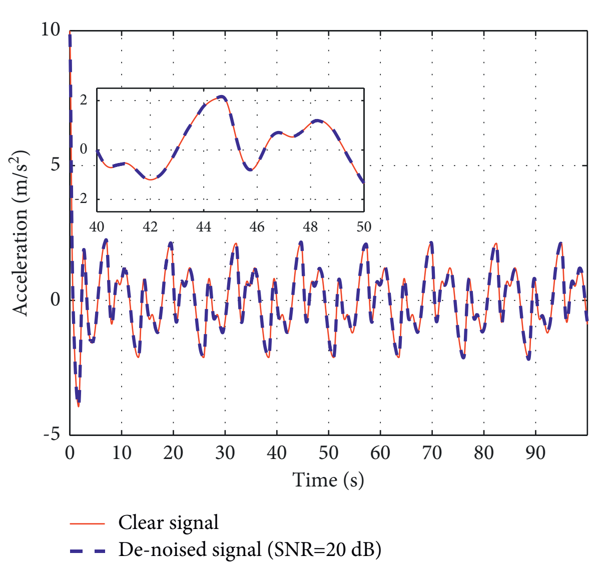

FIGURE 13: Noise elimination of non-linear signal using proposed method when SNR = 50 dB.

Table 2: De-noised results in SNR and RMSE of non-linear signal corrupted by different noise levels.

Noise level	10 dB		15 dB		20 dB	
Criteria	SNR (dB)	RMSE	SNR (dB)	RMSE	SNR (dB)	RMSE
Wavelet shrinkage method	21.631	0.1016	26.364	0.0589	30.368	0.0372
EMD-SG method	17.832	0.1574	22.832	0.0885	27.832	0.0498
Proposed method	24.752	0.0709	29.272	0.0422	33.667	0.0254

Figure 10, which shows that the discrepancies are more obvious compared with non-stationary example.

For the non-linear signal, applying the proposed method to the signal corrupted by the noises with SNRs of 10 dB, 15 dB, and 20 dB, the comparisons of de-noised and clear signals are plotted in Figures 11–13, which show that the de-noised signals are all consistent with the clear signal.

The quantitative analysis is also carried out in the example, and the results are listed in Table 2. Based on the analysis, one can learn that the proposed method is superior to the other two methods when dealing with the non-linear signal corrupted by the noises with SNRs of 10 dB, 15 dB, and 20 dB. At the same time, the SNRs are raised 14.752 dB, 14.272 dB, and 13.667 dB when using the proposed method to eliminate the above corresponding noises, and the RMSEs are reduced 30.22%, 28.35%, and 31.72% compared with the better traditional method (wavelet shrinkage).

5. Conclusion

In this paper, a moving-average method based on complex exponential decomposition is proposed aiming at non-stationary and/or non-linear signal de-noising. The method applies a moving window separating the signal into the small segments and dealing with the segments as stable signals. The time-domain method avoids the shortage of linear methods, and overcomes the limitation of Fourier transform when using Fourier filters. To investigate the performance of the proposed method, numerical study is implemented. The white Gaussian noise is added to clear signal to simulate the noise during signal collection. Two signals, a non-stationary and a non-linear signal, are researched in this paper, which are added noises with SNRs of 10 dB, 15 dB, and 20 dB. Wavelet shrinkage and EMD-SG methods are used to eliminate the noise contained in signal, which shows that the EMD-SG method has better de-noising effect when dealing with non-stationary signal, while the wavelet shrinkage method is better than EMD-SG method when dealing with non-linear signal. Compared with the two methods, the proposed method obtains better results no matter for disposing non-stationary or non-linear signal. The proposed method improves the SNRs by 14.724 dB, 14.428 dB, and 14.688 dB, and reduces RMSEs by 53.56%, 51.99%, and 53.54% compared with EMD-SG method when the non-stationary signal is corrupted by 2%, 5%, and 10% noise. While dealing with the non-linear signal corrupted by 2%, 5%, and 10% noise applying the proposed method, the SNRs are raised 14.752 dB, 14.272 dB, and 13.667 dB, and the RMSEs are reduced 30.22%, 28.35%, and 31.72% compared with wavelet shrinkage method.

Data Availability

The data used to support the findings of this study are available from the corresponding author upon request.

Conflicts of Interest

The authors declare that they have no conflicts of interest.

Acknowledgments

The authors wish to acknowledge the financial support of the National Natural Science Foundation of Zhejiang Province (No. LQ21E090010), the National Natural Science Foundation of China (No. 52001126), the Open Fund of Key Laboratory of Far-shore Wind Power Technology of Zhejiang Province (No. ZOE2021003), the Guangdong Basic and Applied Basic Research Foundation (No. 2022A1515010453), and the State Key Laboratory of Coastal and Offshore Engineering at Dalian University of Technology (No. LP2102).

References

[1] O. E. Esu, Y. Wang, and M. K. Chryssanthopoulos, “Local vibration mode pairs for damage identification in axisymmetric tubular structures,” *Journal of Sound and Vibration*, vol. 494, Article ID 115845, 2021.

[2] S. Wu, W. Xing, Y. Liu, and Y. Shao, “Research on dynamic characteristics and identification method of local defect on the roll surface,” *Engineering Failure Analysis*, vol. 121, Article ID 105063, 2021.

[3] R. Hou and Y. Xia, “Review on the new development of vibration-based damage identification for civil engineering structures: 2010-2019,” *Journal of Sound and Vibration*, vol. 491, Article ID 115741, 2021.

[4] H. Chen, N. Hu, Z. Cheng, L. Zhang, and Y. Zhang, “A deep convolutional neural network based fusion method of two-direction vibration signal data for health state identification of planetary gearboxes,” *Measurement*, vol. 146, pp. 268–278, 2019.

[5] X. Dong, J. Lian, H. Wang, T. Yu, and Y. Zhao, “Structural vibration monitoring and operational modal analysis of offshore wind turbine structure,” *Ocean Engineering*, vol. 150, pp. 280–297, 2018.

[6] Z. Wu and N. E. Huang, “A study of the characteristics of white noise using the empirical mode decomposition method,” *Proceedings of the Royal Society of London. Series A: Mathematical, Physical and Engineering Sciences*, vol. 460, no. 2046, pp. 1597–1611, 2004.

[7] V. Ondra, I. A. Sever, and C. W. Schwingshackl, “Identification of complex non-linear modes of mechanical systems using the Hilbert-Huang transform from free decay

responses," *Journal of Sound and Vibration*, vol. 495, Article ID 115912, 2021.

[8] Y. D. Zhang, X. L. Yang, F. L. Zhu et al., "Characteristics of non–linear dynamics and energy transfer in a vibration gas–solid fluidized bed by using Hilbert–Huang transform," *Powder Technology*, vol. 344, pp. 970–980, 2019.

[9] T.-L. Huang, M.-L. Lou, H.-P. Chen, and N.-B. Wang, "An orthogonal Hilbert-Huang transform and its application in the spectral representation of earthquake accelerograms," *Soil Dynamics and Earthquake Engineering*, vol. 104, pp. 378–389, 2018.

[10] N. E. Huang, Z. Shen, and S. R. Long, "A new view of nonlinear water waves: the Hilbert spectrum," *Annual Review of Fluid Mechanics*, vol. 31, no. 1, pp. 417–457, 1999.

[11] A. González and H. Aied, "Characterization of non-linear bearings using the Hilbert-Huang transform," *Advances in Mechanical Engineering*, vol. 7, no. 4, Article ID 168781401558212, 2015.

[12] A. O. Boudraa, J. C. Cexus, and Z. Saidi, "EMD-based signal noise reduction," *World Acad Sci Eng Tec*, vol. 1, no. 2, pp. 589–592, 2007.

[13] A. V. Oppenheim, W. S. Ronald, and J. R. Buck, *Discrete-Time Signal Processing*, Prentice-Hall, Upper Saddle River, NJ, USA, 1999.

[14] J. G. Proakis and D. G. Manolakis, *Digital Signal Processing: Principles, Algorithms, and Applications*, Prentice-Hall, Saddle River, NJ, USA, 3rd edition, 1996.

[15] D. L. Donoho and I. M. Johnstone, "Ideal spatial adaptation by wavelet shrinkage," *Biometrika*, vol. 81, no. 3, pp. 425–455, 1994.

[16] D. L. Donoho, "De-noising by soft-thresholding," *IEEE Transactions on Information Theory*, vol. 41, no. 3, pp. 613–627, 1995.

[17] N. E. Huang, Z. Shen, S. R. Long et al., "The empirical mode decomposition and the Hilbert spectrum for nonlinear and non-stationary time series analysis," *Proceedings of the Royal Society of London. Series A: Mathematical, Physical and Engineering Sciences*, vol. 454, no. 1971, pp. 903–995, 1998.

[18] P. Flandrin, G. Rilling, and P. Goncalves, "Empirical mode decomposition as a filter bank," *IEEE Signal Processing Letters*, vol. 11, no. 2, pp. 112–114, 2004.

[19] Z. Wu and N. E. Huang, "Ensemble empirical mode decomposition: a noise-assisted data analysis method," *Advances in Adaptive Data Analysis*, vol. 01, no. 01, pp. 1–41, 2009.

[20] N. Rehman and D. P. Mandic, "Filter bank property of multivariate empirical mode decomposition," *IEEE Transactions on Signal Processing*, vol. 59, no. 5, pp. 2421–2426, 2011.

[21] Y.-x. Li and L. Wang, "A novel noise reduction technique for underwater acoustic signals based on complete ensemble empirical mode decomposition with adaptive noise, minimum mean square variance criterion and least mean square adaptive filter," *Defence Technology*, vol. 16, no. 3, pp. 543–554, 2020.

[22] H. Li, Z. Li, and W. Mo, "A time varying filter approach for empirical mode decomposition," *Signal Processing*, vol. 138, pp. 146–158, 2017.

[23] N. Iqbal, A. Zerguine, S. Kaka, and A. Al-Shuhail, "Automated SVD filtering of time-frequency distribution for enhancing the SNR of microseismic/microquake events," *Journal of Geophysics and Engineering*, vol. 13, no. 6, pp. 964–973, 2016.

[24] N. Iqbal, E. Liu, J. H. McClellan, A. Al-Shuhail, S. I. Kaka, and A. Zerguine, "Detection and denoising of microseismic events using time-frequency representation and tensor decomposition," *IEEE Access*, vol. 6, Article ID 22993, 2018.

[25] S. L. James Hu, W.-L. Yang, and H.-J. Li, "Signal decomposition and reconstruction using complex exponential models," *Mechanical Systems and Signal Processing*, vol. 40, no. 2, pp. 421–438, 2013.

[26] F. Liu, H. Li, W. Wang, W. Li, and B. Wang, "Frequency variation and sensor contribution assessment: application to an offshore platform in the South China Sea," *Journal of Sound and Vibration*, vol. 337, pp. 218–232, 2015.

[27] G. H. Golub and C. F. V. Loan, *Matrix Computations*, Johns Hopkins University Press, Baltimore, MD, USA, 3rd edition, 1996.